

The reduction of nitrobenzene as catalyzed by poly(4-vinylpyridine)-immobilized [Rh(COD)(amine)₂](PF₆) complexes under WGSR conditions

A.J. Pardey^{a,*}, M. FernandezFernández^a, J. Alvarez^a, C. Urbina^a, D. Moronta^b,
V. Leon, C. Longo^c, P.J. Baricelli^d, S.A. Moya^e

^a Escuela de Química, Facultad de Ciencias, Universidad Central de Venezuela, Caracas 1020-A, Venezuela

^b Escuela de Física, Facultad de Ciencias, Universidad Central de Venezuela, Caracas 1020-A, Venezuela

^c Centro de Investigación y Desarrollo de Radiofármacos, Facultad de Farmacia, Universidad Central de Venezuela, Caracas, Venezuela

^d Centro de Investigaciones Químicas, Facultad de Ingeniería, Universidad de Carabobo, Valencia, Venezuela

^e Departamento de Química Aplicada, Facultad de Química y Biología, Universidad de Santiago de Chile, Casilla 307-2, Santiago, Chile

Received 4 January 2000; received in revised form 4 May 2000; accepted 4 May 2000

Abstract

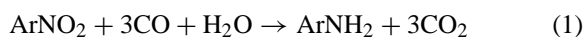
Catalysts for the selective reduction of nitrobenzene to aniline prepared from poly(4-vinylpyridine) (P(4-VP))-immobilized [Rh(COD)(amine)₂](PF₆) (COD=1,5-cyclooctadiene, amine=4-picoline, 3-picoline, 2-picoline, pyridine, 3,5-lutidine or 2,6-lutidine) complexes in contact with 80% aqueous 2-ethoxyethanol, 1×10^{-4} mol Rh/0.5 g of polymer, 0.9 atm of CO pressure at 100°C under water–gas shift reaction conditions (WGSR, CO+H₂O → CO₂+H₂) are described. Aniline production (milimole/3 h) depends on the nature of the amine and decreases in the following order: 2-picoline (0.65)>4-picoline (0.59)≥3-picoline (0.56)>pyridine (0.49)>3,5-lutidine (0.38)>2,6-lutidine (0.34). The immobilized [Rh(COD)(2-picoline)₂](PF₆) complex was found to be reusable as a catalyst for the title reaction. The Rh/2-picoline complex was immobilized to the pyridine groups of the organic polymer as supported by Fourier transform infrared (FT-IR), electron paramagnetic resonance (EPR), X-ray photoelectron spectroscopy (XPS), UV/Vis/diffuse reflectance (DR) spectroscopies, and scanning electron microscopy (SEM) studies. © 2000 Elsevier Science B.V. All rights reserved.

Keywords: Nitrobenzene; WGSR; Rhodium complexes; Poly(4-vinylpyridine); XPS

1. Introduction

The syntheses of aminoarenes compounds (ArNH₂) have aroused a great interest in the industrial manufacture and laboratory use in the production of polyurethanes, dyes, and other chemicals [1]. A convenient method to obtain these nitroarenes is

the catalytic carbonylative reduction of nitroarenes (ArNO₂, Eq. 1) by the use of the CO/H₂O couple [2–14].



Cross-linked polymers have been largely used to immobilize transition metal catalysts. These supports can be functionalized to give ligands for attaching transition metal complexes through coordination bonds. The main goal of this approach is the preparation of catalytic systems displaying the good activity,

* Corresponding author. Fax: +58-2-481-8723.

E-mail addresses: apardey@strix.ciens.ucv.ve (A.J. Pardey), leonv@pdvsa.com (V. Leon).

selectivity and reproducibility, typical of homogeneous catalyst, combined with the easy separation and recovery characteristic of heterogeneous catalyst [15].

A recent review by Nomura [16] deals in part with nature of metallic active species formed during the reduction of aromatic nitro compounds with CO and H₂O by transition metal catalyst. A multi-step catalytic reduction scheme for the reduction of nitrobenzene to aniline has been proposed, in which nitrobenzene cycloaddition to a metal carbonyl complex is an important first step. In this regard, Skoog et al. [17] carried out the characterization and the kinetic studies related to the reaction between nitroarenes (ArNO₂) and Ru(dppe)(CO)₃ where dppe=1,2-bis(diphenylphosphino)ethane. Their kinetics results show a first order reaction in each reagent and an electron transfer process was proposed. Further, an intermediate, identified as Ru(dppe)(CO)₂(η²-ONAr) was formed. The stability of this species is greatly enhanced by the presence of electron-withdrawing substituents on the nitroaromatic compound. Also, the transition state of the rate-determining step was proposed to involve an interaction between the intermediates [ArNO₂]⁻ and [Ru(dppe)(CO)₃]⁺.

In this paper, related to the catalytic reduction of nitrobenzene by [Rh(COD)(amine)₂](PF₆) complexes, immobilized on poly(4-vinylpyridine) (P(4-VP)) under water–gas shift reaction (WGSR) conditions [18], a different approach to the above-described was used and it consists in changing the electronic nature of metal center through a variation of the nature of the amino ligand, instead of the nitroarene substrate, and monitoring their influence on the catalytic activity. These types of ligands are appropriate for evaluating the effects of changes in the π electronic density and in the steric environment of the heterocyclic amine on the catalytic activity. In addition to the activation studies, the characterization of the immobilized [Rh(COD)(2-picoline)₂](PF₆) catalyst by Fourier transform infrared (FT-IR), electron paramagnetic resonance (EPR), X-ray photoelectron spectroscopy (XPS), UV/Vis/diffuse reflectance (DR), differential thermal analysis–thermogravimetric analysis (DTA–TGA) and scanning electron microscopy (SEM) techniques are reported.

2. Experimental

2.1. Materials

The pyridine, methyl pyridines (4-picoline, 3-picoline and 2-picoline (2-pic)) and the dimethyl pyridines (3,5-lutidine and 2,6-lutidine) were obtained from Aldrich and were distilled from KOH. [Rh(COD)Cl]₂ was obtained from Aldrich. Nitrobenzene (Aldrich) was distilled in H₂SO₄ (1 M) and redistilled in CaCl₂ prior to use. Water was doubly distilled. 2-Ethoxyethanol (Aldrich) was distilled from anhydrous stannous chloride. P(4-VP) 2% cross-linked was used as provided by Reilly Industries. All gases and gas mixtures N₂, CO, H₂, He/H₂ (91.4%/8.6%, v/v), CO/CH₄ (95.8%/4.2%, v/v) and CO/CH₄/CO₂/H₂ (84.8%/5.1%/5.3%/4.8%, v/v) were purchased from BOC Gases and were used as received. The rhodium [Rh(COD)(amine)₂](PF₆) complexes were prepared as reported by Denise and Pannetier [19].

2.2. Instrumentation

Gas samples analyses from catalysis runs were performed as described in detail previously [18,20] on a Hewlett-Packard 5890 Series II programmable (ChemStation) gas chromatograph, fitted with a thermal conductivity detector. The column employed was Carbosieve-B (mesh 80–100), obtained from Hewlett-Packard and using the He/H₂ mixture as the carrier gas. Analyses of liquid phase were done on a Hewlett-Packard 5890 Series II programmable gas chromatograph, fitted with 3% OV-101 Supelcoport (mesh 80–100) column and flame ionization detector using *ortho*-xylene as an internal standard, and identified by co-injection on a Hewlett-Packard 5890 Series II programmable gas chromatograph–mass spectrometer, fitted with Pona capillary column (50 m).

Analyses of Rh concentration in the filtered solution were performed on a GBC Avanta atomic absorption (AA) spectrometer operated in the flame mode. The UV/Vis spectra of the solutions (1 cm quartz cell) and of the solids (Labsphere RSA-PE-20 diffuse reflectance cell) were recorded on a Perkin-Elmer Lambda 10 spectrophotometer. Infrared spectra were recorded on a Perkin-Elmer 1760X-FT spectrophotometer using KBr pellets for solid samples. The scan-

ning electron micrographs were recorded on a Hitachi S-500 microscope with energy dispersive X-ray (EDX) detector. EPR experiments were carried out in a conventional Varian E-line X-band spectrometer, using a rectangular cavity operating in the TE 102 mode. The thermal behavior study was carried on TA Instruments SDT 2960 Simultaneous DTA–TGA analyzer. The determinations of pH were performed on a Denver model Acumet Basic pH-meter.

The chemical states of the rhodium samples were analyzed by XPS. The photoelectron spectra were obtained with a Leybold–Heraeus LH 11 (at a pressure of 5×10^{-8} mbar) system. XPS data were obtained by using a non-monochromatized aluminum-anode X-ray source with constant pass energy of 200 eV. The data were collected by using an interfaced personal computer, and the binding-energy scale was calibrated in reference to the reported value of 284.6 eV for the C 1s peak, unless it is otherwise specified. The accuracy of the binding energies was better than 0.2 eV. The XPS peaks were deconvoluted assuming Gaussian line-type, using a standard statistical package.

2.3. Catalyst preparation

A 0.5-g sample of P(4-VP) and a known amount (1.0×10^{-4} mol) of the rhodium complex $[\text{Rh}(\text{COD})\text{-(amine)}_2](\text{PF}_6)$ were stirred at room temperature for 120 h in 10 ml of 2-ethoxyethanol/ H_2O (8/2, v/v), until almost all the rhodium was extracted by the presence of a colorless clear solution above the polymer beads. The yellow polymer was filtered, washed with 2-ethoxyethanol/ H_2O (5 ml) to remove the unabsorbed rhodium, which concentration was determined by UV/Vis and AA spectroscopies. This procedure allowed to know the amount of rhodium supported by subtraction of the amount of unabsorbed rhodium from the initial rhodium concentration.

2.4. Catalyst testing

Catalytic runs were carried out in all-glass reactor vessels consisting of a 100-ml round bottom flask connected to an “O” ring sealed joint to a two-way Rotoflow Teflon stopcock attached to the vacuum line [10]. In a typical run, the loaded polymer beads and 10 ml of 80% aqueous 2-ethoxyethanol were added to the

glass reactor vessel, then, the solution was degassed by three freeze–pump cycles. The reaction vessel was charged with CO/CH_4 mixture at the desired CO partial pressure (0.7 atm at 25°C, but 0.9 atm at 100°C), then suspended in a circulating thermostated glycerol oil bath set at 100°C. The specified temperature was maintained at $\pm 0.5^\circ\text{C}$ by continuously stirring the oil bath, as well as the reaction mixture, which was provided with a Teflon-coated magnetic stirring bar. After reaching a constant WGS activity [18], a 0.26 ml (2.4×10^{-3} mol) sample of nitrobenzene was added to the reaction vessel. Subsequent to the addition of nitrobenzene, the glass reactor vessel was charged with CO/CH_4 at 0.7 atm partial CO pressure at 25°C and placed in the heated oil bath at 100°C for 3 h. At the end of the reaction time, gas samples (1.0 ml) were removed from the reactor vessel in a manner similar to what is described in detail for the WGS catalytic test [20] and analyzed by GC. Also, liquid samples were removed and analyzed by GC and GC-MS. The CH_4 was used as an internal standard to allow the calculation of absolute quantities of CO consumed and CO_2 produced, during a time interval. In addition, calibration curves were prepared periodically for CO, CH_4 , H_2 and CO_2 , and analyzing known mixtures checked their validities.

3. Results and discussion

3.1. Catalysis studies

Research in our group [18] has shown the catalytic activity on the WGS by Rh(I) amino complexes, $[\text{Rh}(\text{COD})(\text{amine})_2](\text{PF}_6)$ (amine=4-picoline, 3-picoline, 2-picoline, pyridine, 3,5-lutidine or 2,6-lutidine), immobilized on 0.5 of P(4-VP) in contact with 10 ml of 80% aqueous 2-ethoxyethanol, $[\text{Rh}]=1.9 \text{ wt.}\%$, under 0.9 atm of CO at 100°C. For example, the WGS catalytic activity, defined as hydrogen turnover frequencies ($TF(\text{H}_2)=\text{mol H}_2 (\text{mol Rh})^{-1} (24 \text{ h})^{-1}$), followed the order: 4-picoline (11.9)>3-picoline (9.9)>2-picoline (5.7)>pyridine (5.4)>3,5-lutidine (5.2)>2,6-lutidine (3.3), under the above-described reaction conditions. The catalytic activity observed in these systems could be explained in terms of a fine balance between electronic and steric effects introduced by the methyl groups. For exam-

ple, 4-picoline ligand system displayed the highest activity. However, reaction rates decreased with increasing steric hindrance on amine, as shown by the lower activity of the 2,6-lutidine (2,6-lutidine is more basic than 4-picoline, however, 2,6-lutidine ligand system is less active, which could be the consequence of the two methyl groups providing steric constraints and, consequently, decreasing the catalytic activity). In these cases, the sterical factor predominates over the electronic influence. These kinds of behavior have also been observed in the homogeneous catalysis of the WGS by systems based on $\text{RhCl}_3 \cdot 3\text{H}_2\text{O}$ [20], $\text{CuCl}_2 \cdot 2\text{H}_2\text{O}$ [21] and *cis*- $[\text{Ir}(\text{CO})_2(\text{amine})_2](\text{PF}_6)$ [22] in aqueous pyridine and substituted pyridines.

The same WGS catalysts, based on Rh(I) complexes immobilized on P(4-VP) in contact with 80% aqueous 2-ethoxyethanol (CO solubility in 2-ethoxyethanol (2.5×10^{-3} mol/l) is higher than the one in water (9.5×10^{-4} mol/l)). The reported values of the solubility of CO in pure solvent at 298 K are estimated according to the solution theory [23], and published parameters [24] also generate a catalytic system, which shows activity on the selective carbonylative reduction of nitrobenzene to aniline under CO (0.9 atm)/ H_2O conditions at 100°C as shown as follows.

For this system, the effects of varying the nature of amine ligand were explored. These results are summarized in Table 1 and they represented the average value of duplicate runs derived for the same experimental conditions. Also, the AA measurement values reveal that the anchoring of the rhodium complexes on 0.5 g

of P(4-VP) is greater than 99% ($[\text{Rh}] = 2.0$ wt.%). The calculated catalytic activity defined as aniline turnover frequencies ($TF(\text{aniline}) = \text{mol aniline} (\text{mol Rh})^{-1} (24 \text{ h})^{-1}$) was reproducible within less than 10% for a series of experimental runs. In addition, formation of aniline, the only organic product (detected by analyzing the catalysis liquid phase), and CO_2 , the only gas product (detected by analyzing the catalysis gas phase), matched stoichiometrically as required by Eq. 1. For example, the average of two replicate values of aniline determined by GC-analyses of the liquid phase (*ortho*-xylene was used as internal standard) and CO_2 determined by GC-analyses of the gas phase (methane was used as internal standard) were 1.95 ± 0.20 and 0.63 ± 0.06 , respectively ($\text{CO}_2/\text{aniline}$ ca. 3.1), for the Rh(2-pic)/P(4-VP) under similar experimental conditions as described in Table 1.

Due to the simplicity and speed of the analysis of gaseous samples, results reported in Table 1 are based on millimole aniline, formed on the basis of CO_2 production, and these were periodically confirmed by analyzing the liquid phase. We had previously reported in detail the consistency of this analytical method [10].

The GC-MS and GC results show that aniline is obtained with selectivity over 99% at 11–36% nitrobenzene conversion range in 3 h. The aniline production depends on the nature of the amine and decreases in the following order: 2-picoline > 4-picoline \geq 3-picoline > pyridine > 3,5-lutidine > 2,6-lutidine. The positive effect of amine basicity should be noted, nitrobenzene conversion increases with the increase of pKa of the amine ligand

Table 1

Reduction of nitrobenzene with $\text{CO}/\text{H}_2\text{O}$ in the presence of rhodium $[\text{Rh}(\text{COD})(\text{amine})_2](\text{PF}_6)$ complexes immobilized on P(4-VP) in contact with aqueous 2-ethoxyethanol as catalyst precursors^a

Amine (pKa) ^b	Yield of CO_2 (mmol) ^c	Yield of aniline ^c (mmol)	<i>TF</i> (aniline) ^d	Nitrobenzene conversion (%)
Pyridine (5.27)	1.49	0.49	49	18
3-Picoline (5.52)	1.68	0.56	47	22
2-Picoline (5.97)	1.95	0.65	53	25
4-Picoline (6.00)	1.77	0.59	49	23
3,5-Lutidine (6.23)	1.14	0.38	31	14
2,6-Lutidine (6.75)	1.01	0.34	28	13

^a0.5 g of polymer, 0.26 ml of nitrobenzene, 8 ml of 2-ethoxyethanol, 2 ml of H_2O , $[\text{Rh}] = 2.0$ wt.%, $P(\text{CO}) = 0.9$ atm at 100°C and $[\text{nitrobenzene}]/[\text{Rh}] = 25$.

^bRef. [25].

^cAfter 3 h.

^dTurnover frequency = mol aniline (mol Rh)⁻¹ (24 h)⁻¹. Selectivity > 99%.

with the only exception of the 2,6-lutidine, which presents strong steric constraints due to the presence of two methyl groups in *ortho* position to nitrogen atom of the aromatic ring that lowers the catalytic activity. These results suggest a critical steric parameter, which can be viewed as the effect of competition for binding to the catalytic center, which is affected more by steric constraints than by electronic effects. For example, the coordination (cycloaddition) of the nitro group with the catalyst (a crucial first step) [26] can be affected by the presence of these two methyl groups and, consequently, decreasing the catalytic activity.

On the other hand, it cannot be ruled out that the little differences in the reactivity between the catalyst formed from different picolines may be to subtle differences in catalyst preparation.

Surprisingly, the role of coordinate amine in these catalysts is different from that in the WGSR by the same Rh/amine/P(4-VP) system. For example, the sterically hindered 2-picoline, which shows a low catalytic activity for the WGSR, is the most effective ligand for the reduction of nitrobenzene among the amine ligands tested. Similar results were observed in the homogeneous reduction of nitrobenzene by *cis*-[Rh(CO)₂(amine)₂](PF₆) in aqueous pyridine and substituted pyridines under CO [10].

The catalytic activity towards the reduction of nitrobenzene by [Rh(COD)(2-pic)₂](PF₆)/P(4-VP) immobilized system is about 45 times higher than the homogeneous solution formed by [Rh(COD)(2-pic)₂](PF₆) (0.1 mmol) dissolved in 10 ml of aqueous 2-ethoxyethanol (2/8, v/v), which shows a 0.02 mol of aniline formation at [Rh]=10 mM, nitrobenzene/Rh=25, and *P*(CO)=0.9 atm at 100°C.

Furthermore, control experiments show catalytic inactivity towards both WGSR and nitrobenzene reduction when 10 ml of 80% aqueous 2-ethoxyethanol under *P*(CO)=0.9 atm and heated at 100°C for 3 h is tested in the absence of any of the [Rh(COD)(amine)₂](PF₆)/P(4-VP) immobilized complexes. Also, the Rh(amine)/P(4-VP) catalytic system exhibits no WGSR activity (i.e. molecular hydrogen is not formed) in the presence of nitrobenzene. Also, the solution above Rh(2-pic)₂/P(4-VP) solid exhibited no activity toward both WGSR and nitrobenzene reduction when tested in the absence of the loaded aminated P(4-VP). Similar results were observed with other Rh(amine)/P(4-VP) systems.

Further studies related to the influence of the reaction conditions variation (carbon monoxide pressure (0–1.9 atm at 80°C, 100°C and 120°C), rhodium content (0.9–12.2 wt.%) and temperature (70–130°C)) on the catalytic reduction of nitrobenzene to aniline by [Rh(COD)(2-pic)₂](PF₆) immobilized on P(4-VP) in contact with 80% of aqueous 2-ethoxyethanol under WGSRs conditions will be published elsewhere.

3.2. Recycling efficiency of the anchored catalyst

The recycling efficiency of the anchored catalyst was determined by reusing, two more times, the same more active polymer-anchored Rh(2-pic)/P(4-VP) catalyst previously used, and checked its catalytic activity on independent experiments under similar conditions. The results are given in Table 2. No change of the catalytic activity was observed after repetitive use. Also, the solution, left after a catalytic run, was analyzed by AA spectrophotometry, and less than 0.01% of rhodium was detected in this solution. On basis of the above results, it could be concluded that the polymer-immobilized catalyst has a high catalytic stability.

To test the role of CO diffusion rate influence on catalytic activity in these static, unmixed systems, a comparative experiment was carried out, in which a 0.5-g sample of P(4-VP) was placed in direct contact with liquid nitrogen in order to change its surface area. Later, the complex [Rh(COD)(2-pic)₂](PF₆) was anchored on the swollen polymer in a similar way as described in Section 2.4, and its catalytic activity towards nitrobenzene reduction was determined un-

Table 2
Recycling efficiency of nitrobenzene reduction catalysis by [Rh(COD)(2-pic)₂](PF₆) complexes immobilized on P(4-VP) in contact with aqueous 2-ethoxyethanol^a

Used time	Yield of CO ₂ ^b (mmol)	Yield of aniline ^b (mmol)	<i>TF</i> (aniline) ^c
1st	1.95	0.65	53
2nd	1.92	0.64	52
3rd	1.90	0.63	51

^a0.5 g of polymer, 0.26 ml of nitrobenzene, 8 ml of 2-ethoxyethanol, 2 ml of H₂O, [Rh]=2.0 wt.%, *P*(CO)=0.9 atm at 100°C for 3 h and [nitrobenzene]/[Rh]=25.

^bAfter 3 h.

^cTurnover frequency=mol aniline (mol Rh)⁻¹ (24 h)⁻¹. Selectivity > 99%.

der analogous conditions to those of Table 1. The results reveal that non-statistically significant improvement of catalytic activity was noted with the swollen polymer, i.e. the average of three replica values of aniline yield (mmol) determined for the swollen and non-swollen catalysts were 0.54 ± 0.02 and 0.55 ± 0.03 mmol, respectively. These results clearly establish that gas/liquid/solid transport of CO was not rate-limiting in the present case. Similar behavior was observed on the WGS catalysis by $[\text{Rh}(\text{COD})(4\text{-pic})_2](\text{PF}_6)$ complex immobilized on P(4-VP) [18], and the same explanation was given there.

3.3. Characterization of the catalyst

The FT-IR, SEM, EPR, UV/Vis/DR and XPS techniques were used to determine the nature of the more active $[\text{Rh}(\text{COD})(2\text{-pic})_2](\text{PF}_6)/\text{P}(4\text{-VP})$ system before and after the catalytic test. Also, the immobilized catalyst was characterized using DTA–TGA analysis.

The FT-IR spectrum of the recently prepared $[\text{Rh}(\text{COD})(2\text{-pic})_2](\text{PF}_6)$ sample shows bands in the $\nu_{\text{C}=\text{C}}$ (3016 cm^{-1}) and $\nu_{\text{C}-\text{H}}$ (2954 , 2923 , 2886 and 2837 cm^{-1}) region, characteristic of the coordinated COD, before being heterogenised. In contrast, the FT-IR spectrum of the immobilized fresh catalyst $\text{Rh}(2\text{-pic})/\text{P}(4\text{-VP})$ shows no bands in the those regions. The results suggest that the nitrogen-functionalized polymer plays the role of a ligand and substitution of the COD molecule does take place as shown in Eq. 2.

Also, the FT-IR spectrum of a solid sample of $[\text{Rh}(\text{COD})(2\text{-pic})_2](\text{PF}_6)$ shows $\nu_{\text{C}-\text{N}}$ bands at 1607 (s), 1481 (s), 1449 (m) and 1435 (m) cm^{-1} , and the FTIR spectrum of a solid sample of the P(4-VP) polymer shows $\nu_{\text{C}-\text{N}}$ bands at 1597 (vs, broad), 1556 (m), 1494 (m), 1447 (m) and 1414 (vs, broad) cm^{-1} . On the other hand, the FT-IR spectrum of the immobilized fresh catalyst $\text{Rh}(2\text{-pic})/\text{P}(4\text{-VP})$ shows $\nu_{\text{C}-\text{N}}$ bands at 1612 (shoulder), 1599 (s, broad), 1555 (m), 1494 (m), 1447 (m) and 1418 (s, broad) cm^{-1} . The IR spectrum obtained from the subtraction of the FT-IR spectrum of the immobilized fresh catalyst $\text{Rh}(2\text{-pic})/\text{P}(4\text{-VP})$ and the FT-IR spectrum of the P(4-VP) sample shows only two $\nu_{\text{C}-\text{N}}$ bands at 1612 (s) and 1430 (s, broad) cm^{-1} , which correspond to the $\nu_{\text{C}-\text{N}}$ bands of the 2-picoline ligand, coordinated to the rhodium center in the $[\text{Rh}(\text{COD})(2\text{-pic})_2](\text{PF}_6)$

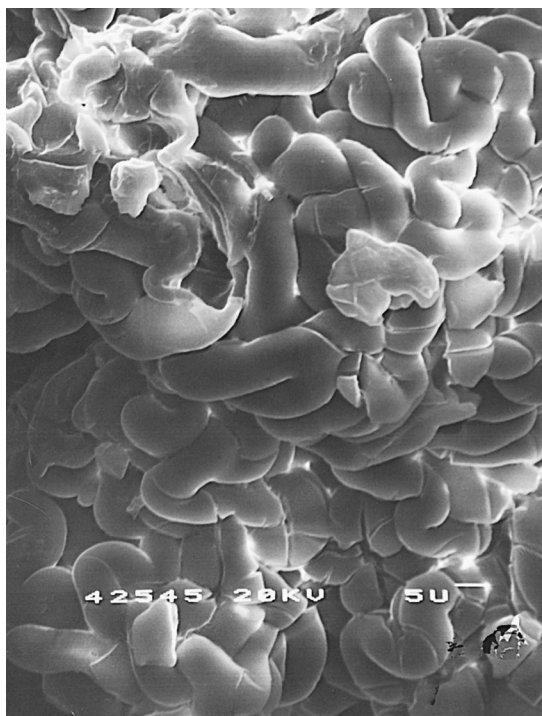


Fig. 1. Scanning electron micrograph of a P(4-VP) sample. Magnification $5000\times$.

complex and they are shifted ca. $\pm 5 \text{ cm}^{-1}$ after the immobilization in the P(4-VP) polymer.

SEM with EDX technique was used for studying the morphology of the solid samples. Fig. 1 shows a SEM micrograph of P(4-VP) sample, from which, it can be observed that the P(4-VP) is formed by agglomerates of grains with smooth surface. Fig. 2 corresponds to the product of the reaction of P(4-VP) with the $[\text{Rh}(\text{COD})(2\text{-pic})_2](\text{PF}_6)$ complex, in contact with aqueous 2-ethoxyethanol after 120 h of continuous stirring in air atmosphere. The observed modifications in some areas on the surface of the polymeric insoluble ligand can be attributed to the anchoring of the rhodium complex, through the pyridine groups of the P(4-VP).

The EPR spectrum of $[\text{Rh}(\text{COD})(2\text{-pic})_2](\text{PF}_6)$ shows no paramagnetic signal, as was expected for this diamagnetic Rh(I) (d^8) compounds (Fig. 3A). The EPR spectrum (Fig. 3B) of a freshly heterogenized sample of $[\text{Rh}(\text{COD})(2\text{-pic})_2](\text{PF}_6)/\text{P}(4\text{-VP})$ shows a paramagnetic signal due to Rh(II) species (d^7), which

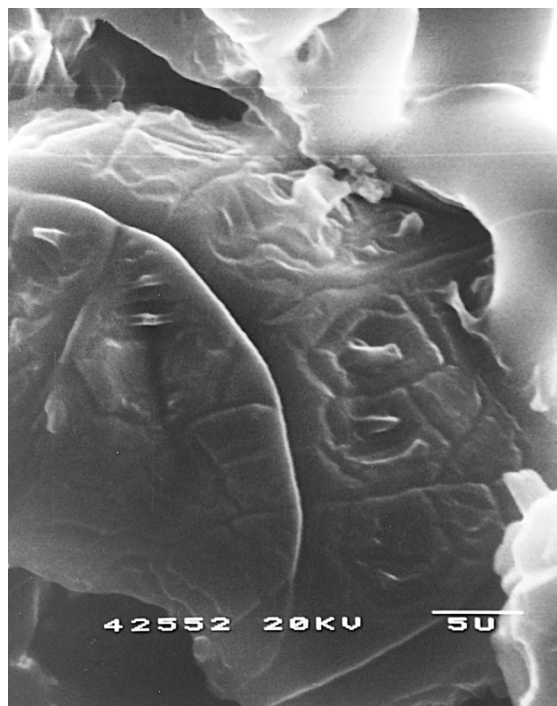


Fig. 2. Scanning electron micrograph of a $[\text{Rh}(\text{COD})(2\text{-pic})_2](\text{PF}_6)/\text{P}(4\text{-VP})$ sample. Magnification 5000 \times .

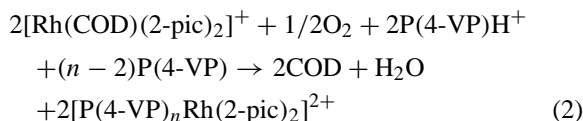
were formed by the oxidation of the Rh(I) precursor in air.

The UV/Vis/DR spectra of the solid samples of $[\text{Rh}(\text{COD})(2\text{-pic})_2](\text{PF}_6)$, before and after being immobilized on the P(4-VP), show a displacement of the d–d transition from 407 (broad peak) to 395 nm. These results indicate a change in the nature of the ligands and in the oxidation states of the precursor $[\text{Rh}(\text{COD})(2\text{-pic})_2](\text{PF}_6)$ after immobilization.

The XPS Rh $3d_{5/2}$ level binding energies of the precursor sample of $[\text{Rh}(\text{COD})(2\text{-pic})_2](\text{PF}_6)$, before and after being immobilized on P(4-VP), and a reference compound are given in Table 3. The deconvoluted XPS spectrum of the $[\text{Rh}(\text{COD})(2\text{-pic})_2](\text{PF}_6)$ after immobilization on P(4-VP) is shown in Fig. 4. The Rh $3d_{5/2}$ level binding energy value of $[\text{Rh}(\text{COD})(2\text{-pic})_2](\text{PF}_6)$ sample is 308.0 eV. Treatment of this Rh(I) complex with P(4-VP) in contact with 2-ethoxyethanol on air caused a 0.4 eV increase in the Rh $3d_{5/2}$ level binding energy, due to the formation of Rh(II). Dennis et al. [27] reported binding energy values for the Rh(II) $3d_{5/2}$ levels in the 308.2–308.5 eV range. In this re-

gard, our value at 308.4 eV appears to be in agreement with those reported. Also, this argument is strongly supported by the EPR data discussed above.

As it is demonstrated in the present study, EPR, UV/Vis/DR, SEM-EDX and XPS results prove the formation of Rh(II) (d^7) due to air oxidation of the Rh(I) (d^8) precursor, which, perhaps, loses its stability by the replacement of the COD ligand by pyridine moieties of the P(4-VP) and leads the formation of rhodium complexes of the type $[\text{P}(4\text{-VP})_n\text{Rh}(2\text{-pic})_2]^{2+}$, as shown in Eq. 2, where P(4-VP) acts as surface-polymer ligand, as well as the proton source, and the value of n remained unknown.



The protonated species $\text{P}(4\text{-VP})\text{H}^+$ came from the hydrolysis of the P(4-VP), which arises by placing the polymer in contact with the aqueous 2-ethoxyethanol solvent system, or from hydrolysis of pyridine residues coming from the P(4-VP) [28]. For example, a freshly prepared solution from $[\text{Rh}(\text{COD})(2\text{-pic})_2](\text{PF}_6)/\text{P}(4\text{-VP})$ in 80% aqueous 2-ethoxyethanol gave a pH 6.89 value, while the solution of the catalytic active system under CO atmosphere gave a lower pH value (6.70). Also, similar SEM and EPR results were observed after immobilization of the Rh(I), *cis*- $[\text{Rh}(\text{CO})_2(4\text{-picoline})_2](\text{PF}_6)$ complex on P(4-VP) in air atmosphere [29]. In this case, the substitution of the two CO ligands by the P(4-VP) nitrogen atoms, as shown by FT-IR data, resulted in air oxidation of the Rh(I) precursor to Rh(II).

The FT-IR spectrum (KBr pellets) of an active Rh(2-pic)/P(4-VP) catalyst sample displays three bands in the ν_{CO} region, two at 1989 and 1961 cm^{-1} (carbonyl-linear Rh species), and one band at 1805 cm^{-1} (carbonyl-bridged Rh species). These data suggest the presence of rhodium carbonyl compounds, anchored to the nitrogen-functionalized polymer as reaction intermediates.

The EPR signal intensity of Rh(2-pic)/P(4-VP) sample exposed to $\text{CO}/\text{H}_2\text{O}$ (Fig. 3C) shows a notorious decrease, probably due to the reduction to non-paramagnetic rhodium species by the $\text{CO}/\text{H}_2\text{O}$ couple. Exposition of the dark solid catalyst to the air by several days causes the disappearance of

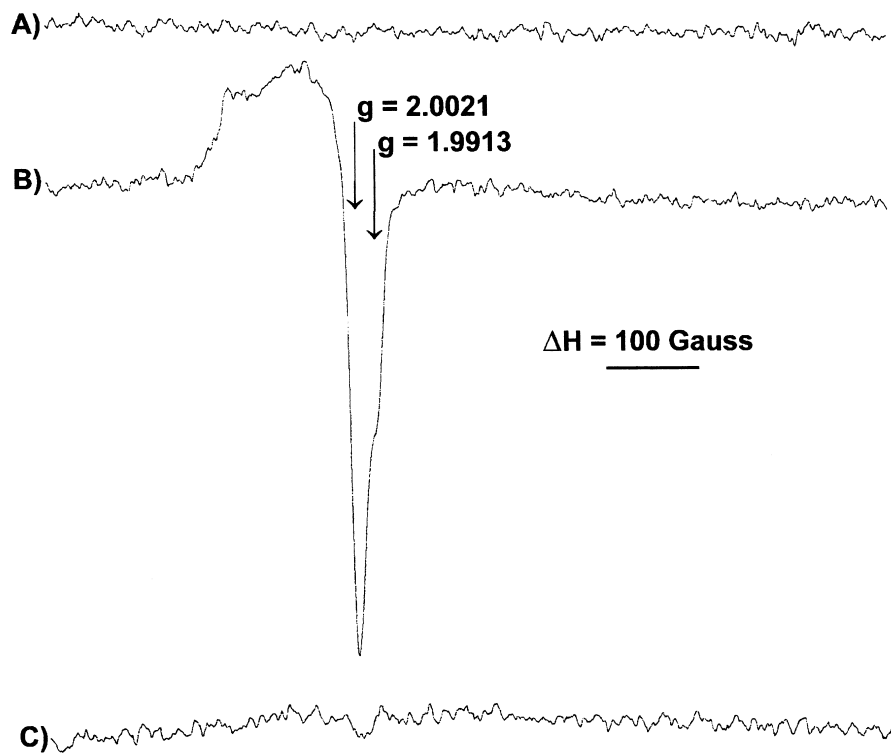


Fig. 3. EPR spectra in the 1250–4000 Gauss region of: (A) $[\text{Rh}(\text{COD})(2\text{-pic})_2](\text{PF}_6)$ complex, (B) $[\text{Rh}(\text{COD})(2\text{-pic})_2](\text{PF}_6)/\text{P}(4\text{-VP})$ fresh catalyst, (C) $[\text{Rh}(\text{COD})(2\text{-pic})_2](\text{PF}_6)/\text{P}(4\text{-VP})$ used catalyst.

the carbonyl bands and the re-establishment of the yellow-colored catalyst precursor. This result reflects the non-stability of these rhodium carbonyl species in the absence of a CO atmosphere. On the other hand, the reversibility of the above behavior, as well as the amine dependency activation results, could rule out the formation of metallic rhodium under reaction conditions. The darkening phenomenon

Table 3
Rh $3d_{5/2}$ binding energies (in eV) and FWHM^a

Compound	Treatment	Rh $3d_{5/2}$
$\text{RhCl}_3 \cdot 3\text{H}_2\text{O}$		309.9 (2.3)
$[\text{Rh}(\text{COD})(2\text{-pic})_2](\text{PF}_6)$	Unsupported	308.0 (2.3)
$[\text{Rh}(\text{COD})(2\text{-pic})_2](\text{PF}_6)/\text{P}(4\text{-VP})$	Fresh catalyst	308.4 (2.6)
$[\text{Rh}(\text{COD})(2\text{-pic})_2](\text{PF}_6)/\text{P}(4\text{-VP})$	Used catalyst	307.0 (3.9)
		308.2 (4.0)

^aBinding energies referenced to O 1s 531.9 eV, a better choice due to the presence of different carbons. FWHM=full width at half maximum, in parentheses.

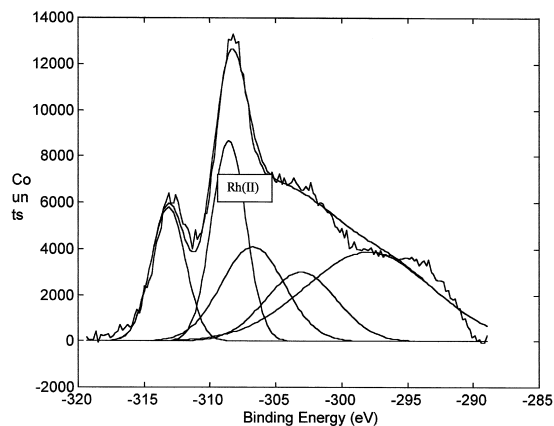


Fig. 4. Curve-fitting of the XPS region including the Rh $3d_{5/2}$ line. The sample corresponds to the $[\text{Rh}(\text{COD})(2\text{-pic})_2](\text{PF}_6)/\text{P}(4\text{-VP})$ fresh catalyst (10% Rh content).

was also observed in the homogeneous catalysis of both WGS [20,30,31] and nitrobenzene reduction [10] by *cis*-[Rh(CO)₂(amine)₂](PF₆). In fact, Fachinetti et al. [31,32] demonstrated that the complexes [Rh₅(CO)₁₃(py)₂]⁻, *cis*-[Rh(CO)₂(py)₂]⁺ and [Rh(CO)(py)₃]⁺ are the active species and responsible for the darkening of the catalytic homogeneous solutions. Also, these results are similar to those of Mattera et al. [33] who observed the formation of different rhodium carbonyl species in the reaction of rhodium sulfonated linear polystyrene with CO and H₂O.

The XPS result and the spectrum of the sample of [Rh(COD)(2-pic)₂](PF₆)/P(4-VP) after being used as a catalyst for the WGS are given in Table 3 and Fig. 5. Two Rh 3d_{5/2} level binding energy values at 308.2 and 307.0 eV are observed. The Rh 3d_{5/2} level binding energy value at 308.2 eV is close to that of the precursor Rh(I). On the other hand, Rh 3d_{5/2} level binding energy at 307.0 eV indicates the presence of a more reduced rhodium species, i.e. (0) or (-1). In addition, Fachinetti et al. [31] have demonstrated the disproportionation of polynuclear carbonyl Rh(0) complexes to Rh(I) and Rh(-I) by pyridine under CO atm. We believe that the same disproportionation reaction takes place with the Rh/P(4-VP) in contact with aqueous 2-ethoxyethanol under CO atmosphere. When the Rh(II)/P(4-VP) immobilized complex is reduced to Rh(0) amino-carbonyl species by the CO/H₂O mixture, disproportionation of this

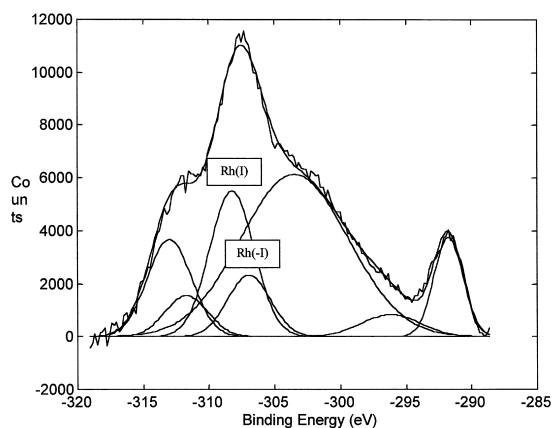


Fig. 5. Curve-fitting of the XPS region including the Rh 3d_{5/2} line. The sample corresponds to the [Rh(COD)(2-pic)₂](PF₆)/P(4-VP) used catalyst (10% Rh content).

Rh(0) species to Rh(I) and Rh(-I) states, assisted by the pyridine residues of P(4-VP), occurs in some extent.

Also, the 0.2-eV difference in the binding energy of Rh 3d_{5/2} level of the Rh(I) [Rh(COD)(2-pic)₂]⁺PF₆ unsupported complex 308.0 eV is very close to the value 308.2 eV for the used catalyst (which contains Rh(I) species). This difference (even though it is within the accuracy of the resolution of the XPS spectrometer) is the result of a change in the electron environment around the Rh(I) atom due to the removal of the COD ligand, under the conditions imposed by the reaction and to some rearrangement of the ligands of the immobilized complex. In addition, it cannot rule out that the presence of small amounts of metallic Rh particles on the surface of the pyridine polymer could change the binding energy of Rh 3d_{5/2} levels.

Based on the diminished EPR signal (Fig. 4), the XPS Rh 3d_{5/2} values at 308.2 and 307.0 eV, the presence of ν_{CO} bands in the FT-IR spectrum of the used catalyst and the results of Fachinetti et al. [31], we propose the presence of both cationic mononuclear and anionic polynuclear amino-carbonyl Rh immobilized complexes as the principal catalytic species on the used catalyst, the latter species bearing bridging carbonyls bonds (ν_{CO} band at 1805 cm⁻¹).

The DTA–TGA data show that the immobilized catalyst is stable at 250°C, however, a weight loss was observed around 100°C, due to the moisture content coming from the preparative method. The result is shown in Fig. 6. After 130°C, the weight loss in the immobilized catalysts might be due to the degrada-

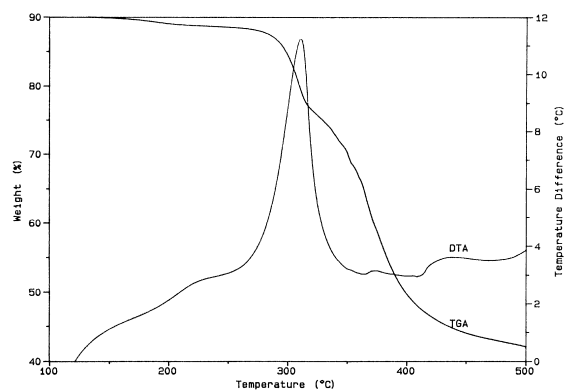


Fig. 6. DTA–TGA curves for a heterogenized [Rh(COD)(2-pic)₂](PF₆)/P(4-VP) sample.

tion of polynuclear carbonyl to mononuclear carbonyl anchored-rhodium species.

4. Conclusions

The following conclusions have been drawn from the catalytic and characterization studies of the nitrobenzene reduction by Rh(I) amino complexes immobilized on aminated polymer P(4-VP) in contact with aqueous 2-ethoxyethanol under conditions analogous to those for the WGS. These catalytic systems are very stable and selective (aniline was the principal organic product observed with a 99% selectivity), and among the catalysts studied, [Rh(COD)(2-pic)₂](PF₆)/P(4-VP) system appears to be the most active. The FT-IR, UV/Vis/DR, EPR, SEM, XPS and DTA–TGA data of the Rh(2-pic)/P(4-VP) system suggest the presence of immobilized rhodium carbonyl compounds with different nuclearities and different oxidation states anchored to the nitrogen-functionalized polymer as catalytic reaction intermediates.

Acknowledgements

The present work was carried out under the research programs CONICIT-Venezuela (Proy. S1-95001662). We thank Reilly Industries by donating the P(4-VP) cross-linked polymer (lot no. 70515AA). Also, we thank Prof. Mireya R. Goldwasser, (Universidad Central de Venezuela) for helpful discussions and Juan Carlos de Jesús (PDVSA-INTEVEP) for XPS measurements and advice.

References

- [1] D.M. Samuel, *Industrial Chemistry — Organic*, Royal Institute of Chemistry, Monographs for Teachers No. 11, London (1972) 117.
- [2] P. Escaffre, A. Thorey, P. Kalck, *J. Mol. Catal.* 33 (1985) 87.
- [3] R.A. Sánchez-Delgado, A.A. Oramas, *J. Mol. Catal.* 36 (1986) 283.
- [4] K. Nomura, M. Ishino, M. Hazama, *J. Mol. Catal.* 66 (1991) L1.
- [5] F. Ragaini, S. Cenini, S. Tollari, *J. Mol. Catal.* 85 (1993) L1.
- [6] K. Kaneda, H. Kuwahara, T. Imanaka, *J. Mol. Catal.* 8 (1994) L267.
- [7] F. Ragaini, M. Pizzotti, S. Cenini, A. Abboto, G.A. Pagani, F. Demartin, *J. Organomet. Chem.* 489 (1996) 107.
- [8] K. Nomura, *J. Mol. Catal. A* 95 (1995) 203.
- [9] F. Ragaini, S. Cenini, *J. Mol. Catal. A* 105 (1996) 145.
- [10] C. Linares, M. Mediavilla, P. Baricelli, C. Longo-Pardey, S.A. Moya, A.J. Pardey, *Catal. Lett.* 50 (1998) 183.
- [11] C. Linares, M. Mediavilla, A.J. Pardey, C. Longo, P. Baricelli, S.A. Moya, *Bol. Soc. Chil. Quim.* 43 (1998) 55.
- [12] M. Mdleleni, R.G. Rinker, P.C. Ford, *J. Mol. Catal.* 89 (1994) 283.
- [13] A.M. Tefesh, M. Beller, *Tetrahedron Lett.* 36 (1995) 9305.
- [14] S.A. Moya, R. Sariago, P. Aguirre, R. Sartori, P. Dixneuf, *Bull. Soc. Chim. Belg.* 104 (1995) 19.
- [15] E.A. Bekturov, S.E. Kudaibergerov, *Catalysis by Polymers*, Huthig, Wepf Zug, Deidelberg, Oxford, CT/USA (1996).
- [16] K. Nomura, *J. Mol. Catal. A* 130 (1998) 1.
- [17] S.J. Skoog, J.P. Campbell, W.L. Gladfelter, *Organometallics* 13 (1994) 4137.
- [18] A.J. Pardey, M. Fernández, M. Canestrari, P. Baricelli, E. Lujano, C. Longo, R. Sartori, S.A. Moya, *React. Kinet. Catal. Lett.* 67 (1999) 325.
- [19] B. Denise, G. Pannetier, *J. Organomet. Chem.* 63 (1973) 423.
- [20] A.J. Pardey, P.C. Ford, *J. Mol. Catal.* 53 (1989) 247.
- [21] M. Mediavilla, D. Pineda, F. López, D. Moronta, C. Longo, S.A. Moya, P. Baricelli, A.J. Pardey, *Polyhedron* 17 (1998) 1621.
- [22] M. Fernández, M. Meza, M. Mediavilla, C. Longo, S.A. Moya, F. López, P. Baricelli, A.J. Pardey, *Anal. Quim. Int. Ed.* 94 (1998) 127.
- [23] J.M. Prausnitz, *Molecular Thermodynamics of Fluid-Phase Equilibria*, Prentice-Hall, Englewood Cliffs, NJ, 1969, Chap. 8.
- [24] *Encyclopedia of Chemical Technology*, 3rd edn. vol. 21 Wiley, New York, 1978, p. 377.
- [25] K. Schofield, in: *Hetero-Aromatic Nitrogen Compounds*, Plenum, New York, 1967, pp. 146–148.
- [26] F. Ragaini, S. Cenini, F. Demartin, *J. Chem. Soc., Chem. Commun.* (1992) 1467.
- [27] A.M. Dennis, R.A. Howard, K.M. Kadish, J.L. Bear, *Inorg. Chim. Acta* 44 (1980) L139.
- [28] Y.E. Kirsch, O.P. Komarova, G.M. Luvokin, *Eur. Polym. J.* 9 (1973) 1405.
- [29] A.J. Pardey, M. Mediavilla, M. Canestrari, C. Urbina, D. Moronta, E. Lujano, P. Baricelli, C. Longo, R. Pastene, S.A. Moya, *Catal. Lett.* 56 (1998) 231.
- [30] B.S. Lima-Neto, K.H. Ford, A.J. Pardey, R.G. Rinker, P.C. Ford, *Inorg. Chem.* 30 (1991) 3837.
- [31] G. Fachinetti, G. Fochi, T. Funaioli, *Inorg. Chem.* 33 (1994) 1719.
- [32] G. Fachinetti, T. Funaioli, P.F. Zanazzi, *J. Organomet. Chem.* 460 (1993) C34.
- [33] V.D. Mattera, P.J. Squattrito, W.M. Risen, *Inorg. Chem.* 23 (1984) 3597.